Atmos. Chem. Phys. Discuss., 14, 8257–8285, 2014
www.atmos-chem-phys-discuss.net/14/8257/2014/
doi:10.5194/acpd-14-8257-2014


Atmospheric Chemistry and Physics Discussions



# Hygroscopic properties of newly formed ultrafine particles at an urban site surrounded by a deciduous forest in northern Japan during the summer of 2011

**J. Jung**[1,*] **and K. Kawamura**[1]

[1]Institute of Low Temperature Science, Hokkaido University, Sapporo 060-0819, Japan
[*]now at: Center for Gas Analysis, Korea Research Institute of Standards and Science, Daejeon 305-340, Korea

Received: 11 March 2014 – Accepted: 18 March 2014 – Published: 25 March 2014

Correspondence to: K. Kawamura (kawamura@lowtem.hokudai.ac.jp)

Published by Copernicus Publications on behalf of the European Geosciences Union.







## Abstract

To investigate the hygroscopic property of ultrafine particles during the new particle formation event, hygroscopic growth factors ($g$(RH)) of size-segregated atmospheric particles were measured at an urban site in Sapporo, northern Japan, during the summer of 2011. Hygroscopic growth factors at 85 % RH ($g$(85 %)) of freshly formed nucleation mode particles were measured at a dry particle diameter ($D_p$) centered at 20 nm to be 1.11 to 1.28 (average 1.16 ± 0.06), which are equivalent to 1.17 to 1.35 (1.23 ± 0.06) for a dry $D_p$ centered at 100 nm after considering the Kelvin effect. These values are comparable with those of secondary organic aerosols, suggesting that low-volatility organic vapors are important to the burst of nucleation mode particles at the measurement site surrounded by a deciduous forest. Gradual increases in mode diameter after the burst of nucleation mode particles were obtained under southerly wind condition with a dominant contribution of intermediately-hygroscopic particles. However, sharp increases in mode diameter were obtained when wind direction shifted to northwesterly or northeasterly with a sharp increase in highly-hygroscopic particle faction in the Aitken mode particles, indicating that local wind direction is an important factor controlling the growth of newly formed particles and their hygroscopic properties. Higher $g$(85 %) values (1.27 ± 0.05) were obtained at a dry $D_p$ of 120 nm when the air masses originated from the Asian Continent, whereas lower $g$(85 %) values (1.19 ± 0.06) were obtained when clean marine air masses arrived at the urban site. These results indicate that the hygroscopic property of large Aitken and small accumulation mode particles (80–165 nm) is highly influenced by the long-range atmospheric transport of particles and their precursors.

## 1 Introduction

New particle formation (NPF) in the atmosphere is an important parameter in governing the radiative forcing by aerosols and cloud formation process. NPF is frequently





ACPD
14, 8257–8285, 2014



occurred worldwide (Kulmala et al., 2004; Holmes, 2007; Bzdek and Johnston, 2010). Recent direct size-segregated observation of the sub-2 nm particles showed that extremely low-volatile organic compounds affect not only nuclei growth but also participate in relatively early stages of the new particle formation process (Kulmala et al., 2013; Ehn et al., 2014). Although important understanding on the nucleation mechanisms and the growth of freshly nucleated particles is advanced more recently (Hegg and Baker, 2009; Metzger et al., 2010; Zhang, 2010; Zhang et al., 2012), detailed nucleation mechanisms in the atmosphere still remain ambiguous.

In a suburban area of the Yangtze River delta in China, Gao et al. (2009) showed that sulfuric acid is important for the initiation of NPF. Yue et al. (2010) observed that the condensation and neutralization of sulfuric acid caused the growth of freshly nucleated particles during sulfur-rich periods in urban Beijing, China, whereas organic compounds were responsible for particle growth during sulfur-poor periods. Cheung et al. (2011) reported that freshly nucleated particles at an urban site in Brisbane, Australia, showed different growth patterns depending on the type of air mass arrived in the measurement site. However, mechanisms for nucleation and growth of freshly nucleated particles in an urban area surrounded by a deciduous forest have been poorly understood.

Because secondary organic aerosols (SOA) and water-soluble inorganic ions such as $(NH_4)_2SO_4$ have different hygroscopic properties, the hygroscopic growth factor ($g$(RH)) of nucleated particles can be used to estimate their chemical compositions. Ehn et al. (2007) measured the $g$(RH) of freshly nucleated particles in a boreal forest in southern Finland. Using hygroscopic growth measurements of size-segregated atmospheric particles, they observed that the $g$(RH) values of nucleated particles decreased as particles grow to the Aitken mode. Ristovski et al. (2010) simultaneously measured the hygroscopicity and volatility of nucleated particles in a eucalypt forest in Australia. They observed that nucleated particles were composed of both sulfate and organics, the latter showed the volatility and hygroscopicity similar to photo-oxidation products of $\alpha$-pinene. However, the chemical and hygroscopic properties of freshly





ACPD
14, 8257–8285, 2014



nucleated particles have rarely been studied, especially in an urban area adjacent to a deciduous forest.

Particle number size distributions were measured at an urban site in Sapporo, northern Japan, using a scanning mobility particle sizer (SMPS) during the summer of 2011 (Jung et al., 2013). They have discussed the factors controlling the burst of nucleation mode particles and their subsequent growth at the urban site. Because the burst of nucleation mode particles are mainly caused by the growth of nucleated clusters (< 1 nm) into a detectable size (> 3 nm), we define particles generated from the burst of nucleation mode particles during the NPF event periods as freshly formed nucleation mode particles. In this study, we investigate the hygroscopic properties of size-segregated atmospheric particles at the same urban site in northern Japan during the summer of 2011 using a hygroscopicity tandem differential mobility analyzer (H-TDMA) and meteorological parameters. The formation process of the nucleation mode particles during the NPF event periods is investigated using their hygroscopic growth factors. The subsequent growth of freshly formed nucleation mode particles to the Aitken mode is also investigated using the size-segregated hygroscopic growth factor and meteorological parameters.

## 2 Experimental

### 2.1 Description of the measurement site

The hygroscopic properties of ultrafine particles were continuously measured at an urban site in Sapporo, northern Japan, during 26 July–9 August 2011 using a hygroscopicity tandem differential mobility analyzer (H-TDMA). An area map of the measurement site is shown in Fig. 1. The concentrations of total suspended particle (TSP) mass, $O_3$, $NO_x$, and $SO_2$ near the urban site were obtained from the Ministry of the Environment of Japan at the Sapporo observatory (http://soramame.taiki.go.jp/). The time shown in this study represents local time in Japan (LT) (GMT + 09:00).





ACPD
14, 8257–8285, 2014



The city of Sapporo (population 1.9 million, area 1121 $km^2$) is located in the western part of Hokkaido, the northernmost main island of Japan (Fig. 1). Sapporo is surrounded by deciduous forested areas with an exception of its northwestern border. The urban site was located at the north campus of Hokkaido University (43°3′56″ N, 141°21′27″ E) in the northwest of downtown Sapporo (Aggarwal and Kawamura, 2009; Kitamori et al., 2009). The campus is surrounded mainly by residential area, and the urban center is located ∼ 2 km south of the university campus.

Aggarwal and Kawamura (2009) found that photochemical aging was an important factor controlling the water-soluble properties of organic aerosols at the same Sapporo urban site during the spring and early summer of 2005. Agarwal et al. (2010) reported that most of dicarboxylic acids, $\alpha$-dicarbonyls, levoglucosan, water-soluble organic carbon (WSOC), and inorganic ions (i.e., $SO_4^{2-}$, $NH_4^+$, and $K^+$) were enriched in fine particles ($PM_{1.1}$) collected at the Sapporo urban site during the summer of 2005. Using particle size distributions during the summer of 2011, Jung et al. (2013) showed that the burst of nucleation mode particles typically started in the morning (07:00–11:30 LT) at the same urban site with simultaneous increases in concentrations of $SO_2$ and $O_3$ and the UV index under clear weather conditions.

### 2.2 Measurement of hygroscopic growth factors of size-segregated ultrafine particles

The hygroscopic growth factors of size-segregated atmospheric particles were measured using the H-TDMA (Mochida and Kawamura, 2004; Jung et al., 2011). The H-TDMA system consisted of a $^{241}$Am neutralizer, two DMAs (TSI, model 3081), an aerosol humidity conditioner (Nafion tubing) and a condensation particle counter (CPC) (TSI, model 3010). Sample and sheath flow rates of two DMAs were set to 0.3 and 3 L $min^{-1}$ (LPM), respectively. Sample inlet was installed at ∼ 5 m height a.g.l. Ambient air was drawn through a $PM_{1.0}$ cyclone inlet with a flow rate of 16.7 L $min^{-1}$. An aliquot





ACPD
14, 8257–8285, 2014



(0.3 L min$^{-1}$) of the sampled air was separated and dried to a relative humidity (RH) < 5 % using two diffusion dryers before being introduced to the H-TDMA.

Dry mobility diameter selected in the first DMA was increased every 5 min (6 diameters from 20 nm to 120 nm with a 20 nm increment) over 30 min. Dry mono-dispersed particles classified in the first DMA was then humidified to 85 % RH using the aerosol humidity conditioner. The size distributions of resulting particles were measured using the second DMA and the CPC. RH in a sheath flow of the second DMA was maintained as 85 %. A residence time of the particles between the aerosol humidity conditioner and second DMA was roughly estimated as 10 s. All H-TDMA experiments were conducted at sampled air temperatures of 287–294 K with a mean of 291 K. The size distribution of humidified particles corrected for diffusion losses in the H-TDMA was fitted using a lognormal Gaussian curve. Since a mode peak diameter (Mode $D_p$) of the Gaussian curve fit was used in this study, broadening effects caused by a transfer function between the first and second DMAs are negligible.

The hygroscopic growth factor ($g$(RH)) of particles is defined as following formula:

$$g(\mathrm{RH}) = \frac{D_p(\mathrm{RH})}{D_p(\mathrm{dry})} \quad (1)$$

where $D_p$(dry) is the dry particle diameter under RH < 5 %, and $D_p$(RH) is its diameter at a specific RH. The $g$(RH) of pure $(NH_4)_2SO_4$ was measured as 1.56 ± 0.01 ($n$ = 3) at 85 % RH, which agrees well with the $g$(85 %) of 1.56 predicted using the thermodynamic aerosol inorganic model (AIM) (Clegg et al., 1998). The predicted $g$(RH) was calculated by considering the Kelvin effect and assuming the density of 1.76 g cm$^{-3}$ and dynamic shape factor ($\chi$) of unity for dry particles.

### 2.3 Meteorological parameters and air mass backward trajectory

Meteorological data (temperature, wind speed, RH, and rainfall) during the urban campaign were obtained from the Japan Meteorological Agency in Sapporo (43°3.6′ N,





ACPD
14, 8257–8285, 2014



141°19.7′ E, 17 m a.g.l.), which is located ∼ 2.6 km south of the urban site. Average ambient temperature and RH were measured as 23 ± 3 °C and 72 ± 11 %, respectively. Most measurements were carried out under clear weather conditions, although a number of rainfall events occurred. Three rainfall events were observed on 27 July, 13:00–14:00 LT, 5 August, 16:00 LT, and 6 August, 16:00 LT. The prevailing local wind directions during the urban campaign varied between southeasterly and northwesterly with an average wind speed of $3 \pm 2\,m\,s^{-1}$ (range: 0–11 $m\,s^{-1}$) (Fig. 1).

Air mass backward trajectory can be utilized to characterize potential source regions and transport pathways of atmospheric particles. Air mass backward trajectories that ended at the measurement site were computed at the heights of 200 m and 500 m above ground level using the HYSPLIT (HYbrid Single-Particle Lagrangian Trajectory) backward trajectory analysis (Draxler and Rolph, 2012; Rolph, 2012). All calculated backward trajectories extended 96 h backward with a 1 h interval. Up to 20 % errors of the traveled distance are typical for those trajectories computed from analyzed wind fields (Stohl, 1998). Thus, calculated air mass pathways indicate the general airflow pattern rather than the exact pathway of an air mass.

## 3 Results and discussion

### 3.1 Overview of hygroscopic growth factors of size-segregated atmospheric particles

Figure 2 shows the number distributions of humidified particles at the dry $D_p$ range of 20–120 nm as a function of $g$(85 %). The number concentrations of nucleation mode (7–30 nm) particles ($N_{nuc}$) are also given in Fig. 2a. During the entire measurement period, eight new particle formation (NPF) events occurred on 27, 31 July, 1–3, 5, 6, and 8 August and are marked as empty white boxes in Fig. 2. A NPF event was defined as a sharp increase in the $N_{nuc}$/number concentration of ultrafine particles ($N_{UFP}$) (7–100 nm) ratios of $> 0.5$ with elevated $N_{UFP}$ (refer to Fig. 3 in Jung et al., 2013).





ACPD
14, 8257–8285, 2014



Increases in the number concentrations of humidified particles at dry $D_p$ = 20 nm were observed during the NPF event periods (Fig. 2b). Increases in the number concentrations of humidified particles at dry $D_p$ = 40 nm were consistent with those at dry $D_p$ = 20 nm with and without a time gap. Variations in the hygroscopicity of freshly formed nucleation mode particles and grown Aitken mode nucleated particles are discussed in Sect. 3.4.

Elevated number concentrations of humidified particles at the dry $D_p$ range of 80–120 nm were observed during 27–29 July and 6–8 August whereas low number concentrations of particles were observed during 30 July–5 August. Variations in the number distributions of humidified particles and $g$(85 %) values at dry $D_p$ = 80 nm were quite similar to those at dry $D_p$ = 120 nm. Elevated number concentrations of smaller particles (dry $D_p$ = 20 nm and 40 nm) were observed during 30 July–5 August due to new particle formation events as shown in Fig. 2a. Increases in number concentrations of larger particles (dry $D_p$ > 80 nm) were also obtained during the same period with some time delay. This can be explained by either condensational growth of newly formed particles or inflow of different air masses due to the change in local wind direction. Characteristics of hygroscopic properties of nucleation and Aitken mode particles during the new particle formation episodes are discussed in Sect. 3.5.

### 3.2 Diel variations in hygroscopic growth factors of size-segregated ultrafine particles

$g$(85 %) of particles at dry $D_p$ of < 100 nm are smaller than those of equivalent larger particles ($D_p$ > 100 nm) due to the Kelvin effect. Because most previous studies measured growth factors of nebulised particles at dry $D_p$ = 100 nm (e.g. Gysel et al., 2004; Sjogren et al., 2008; Jung et al., 2011), $g$(85 %) of particles at dry $D_p$ of < 100 nm were converted to those of equivalent large particles assuming dry $D_p$ = 100 nm. Hereafter, the converted terms are denoted as Equiv. $g$(85 %) at dry $D_p$ = 100 nm. Because $g$(85 %) of dry $D_p$ < 100 nm before correction were similar to those of water-soluble organic aerosols but much lower than those of inorganic compounds such as ammonium





ACPD
14, 8257–8285, 2014



sulfate (Table 1), this study used $g$(RH) curve of water-soluble organic aerosols obtained by Jung et al. (2011). Thus, the conversion was done based on the Köhler equation using the $g$(RH) curve of water-soluble organic aerosols.

Figure 3a shows diel variations in median $g(85\,\%)_{\_total}$ at the dry $D_p$ range of 20–120 nm and $N_{nuc}$ during the NPF event periods. The burst of nucleation mode particles and $g(85\,\%)_{\_total}$ at the dry $D_p$ range of 20–120 nm were characterized by three phases marked as A, B, and C as shown in Fig. 3a. Gradual increase in $N_{nuc}$ and significant decrease in $g(85\,\%)_{\_total}$ values were observed during 05:00–08:00 LT (Phase A) when NO concentrations significantly increased from near zero to ~ 4 ppbv (Fig. 3c). In Phase B, both $N_{nuc}$ and $g(85\,\%)$ values then largely increased during 08:00–10:30 LT with increases in $SO_2$ and $O_3$ concentrations. In Phase C, peak $N_{nuc}$ and relatively constant $g(85\,\%)_{\_total}$ values were observed during 10:30–12:00 LT with continuous increase in $O_3$ concentrations.

During the non-NPF periods (Fig. 3b), $N_{nuc}$ and median $g(85\,\%)_{\_total}$ values at the dry $D_p$ of 20–120 nm showed different diel variations compared to those during the NPF event periods (Fig. 3a). The burst of nucleation mode particles was not observed in the morning. The $g(85\,\%)_{\_total}$ values at the dry $D_p$ range of 20–120 nm gradually decreased during 04:00–11:00 LT when $SO_2$ and NO peaked (Fig. 3d). The decreased $g(85\,\%)_{\_total}$ values with an increase in NO concentrations in the morning suggest that the decrease in $g(85\,\%)_{\_total}$ values during the Phase A period is attributed to increased emissions of water-insoluble ultrafine particles probably from traffic.

Very similar g$(85\,\%)_{_total}$ values at the dry $D_p$ range of 40–120 nm were observed during the Phase A period when the burst of nucleation mode particles occurred (Fig. 3a). However, higher $g(85\,\%)_{\_total}$ values were observed as dry $D_p$ increased during the same time period (05:00–08:00 LT) when the burst of nucleation mode particles did not occur (Fig. 3b). These results imply that water-insoluble particles emitted from traffic may contribute a large portion of particles at the dry $D_p$ range of 40–120 nm during the NPF event periods compared to the non-NPF periods. Thus, water-insoluble particles





ACPD
14, 8257–8285, 2014



from traffic are important in the hygroscopic property of particles at the dry $D_p$ range of 40–120 nm prior to the burst of nucleation mode particles.

The $g(85\,\%)_{\_total}$ values at dry $D_p$ = 20 nm became larger as $N_{nuc}$ increased during the Phase B period when the burst of nucleation mode particles occurred (Fig. 3a), suggesting that freshly formed nucleation mode particles are enriched with water-soluble components. Simultaneous increases in $g(85\,\%)_{\_total}$ values at the dry $D_p$ range of 40–120 nm were observed during the Phase B periods with increases in $O_3$ and $SO_2$ concentrations. The increased $g(85\,\%)$ values can be explained by the subsequent growth of freshly formed nucleation mode particles to the Aitken mode or by condensation of water-soluble inorganic compounds or organic vapors onto pre-existing Aitken mode particles. Almost constant $g(85\,\%)_{\_total}$ values were obtained at the dry $D_p$ of 20–120 nm when $N_{nuc}$ maximized during the Phase C period (Fig. 3a).

### 3.3 Categorization of hygroscopic properties of ultrafine particles

Particle number distributions as a function of $g(85\,\%)$ values generally exhibited unimodal or bimodal distributions as shown in Fig. 4. Freshly formed nucleation mode particles typically showed a unimodal distribution (Fig. 2b). Based on the number distributions of humidified particles as a function of $g(85\,\%)$, particle distributions were divided into three categories: less-, intermediately-, and highly-hygroscopic fractions. Particle number distributions are shown in Fig. 4 as a function of $g(85\,\%)$ for 5 August, 16:00–17:00 LT at dry $D_p$ = 100 nm, 5 August, 09:00–10:00 LT at dry $D_p$ = 20 nm, and 28 July, 20:00–21:00 LT at dry $D_p$ = 120 nm as typical examples for less-, intermediately- and highly-hygroscopic particles, respectively. $g(85\,\%)$ at dry $D_p$ = 20 nm was converted to Equiv. $g(85\,\%)$ of dry $D_p$ = 100 nm by considering the Kelvin Effect. Two thresholds were chosen as $g(85\,\%)$ of 1.08 for the separation of less- and intermediately-hygroscopic fractions and of 1.25 for separation of intermediately- and highly-hygroscopic fractions. Number fractions of three hygroscopic categories were calculated using these two threshold values. Mochida et al. (2008) used similar threshold values of 1.11 and 1.29 for the separation of three hygroscopic fractions.





ACPD
14, 8257–8285, 2014



The $g$(85 %) values of water-soluble inorganic ions are generally higher than 1.5 (Jung et al., 2011). It is well known that elemental carbon, crustal elements, and water-insoluble organics have $g$(85 %) values of ∼ 1. Because the size of crustal elements is generally larger than 100 nm, the less-hygroscopic ultrafine particles in the urban atmosphere can be attributed to elemental carbon and water-insoluble organic aerosols (Kuwata et al., 2007). The $g$(85 %) values of water-soluble organics are obtained as ∼ 1.1–2.2 (Virkkula et al., 1999; Saathoff et al., 2003; Sjogren et al., 2008; Jung et al., 2011). Thus, intermediately-hygroscopic particles can be attributed to water-soluble SOA, including a small fraction of water-soluble primary organic aerosols. Because elevated levels of intermediately-hygroscopic particles were typically observed during the NPF event periods, freshly formed nucleation mode particles may contain abundant amounts of water-soluble SOA. Peak number concentrations of highly-hygroscopic particles were obtained at $g$(85 %) of ∼ 1.4. Because this $g$(85 %) value is lower than those of water-soluble inorganic ions such as ammonium sulfate, highly-hygroscopic particles can be attributed to a mixture of secondary organic aerosols and inorganic ions.

### 3.4 Hygroscopic growth factors of freshly formed nucleation mode particles during the NPF events

A mode peak diameter (Mode $D_p$) was obtained from a lognormal Gaussian fit of particle number size distribution smaller than 100 nm. The Mode $D_p$ of freshly formed nucleation mode particles was obtained from particle number size distributions averaged over one hour period from the beginning of the burst of nucleation mode particles. Similarly, the Mode $D_p$ of grown Aitken mode nucleated particles was obtained from particle number size distribution averaged over one hour period before the end of a linear growth of the Mode $D_p$ of freshly formed nucleation mode particles (Jung et al., 2013). The Mode $D_p$ of freshly formed nucleation mode particles ranged from 12 nm to 24 nm with an average of 16 ± 3 nm, whereas the Mode $D_p$ of particles after particle growth ranged from 38 nm to 48 nm with an average of 44 ± 5 nm (Table 1). Because average Mode $D_p$ values of freshly formed nucleation mode particles and grown Aitken





ACPD
14, 8257–8285, 2014



mode nucleated particles were close to 20 nm and 40 nm, respectively, $g(85\,\%)$ values at dry $D_p$ of 20 nm and 40 nm were used to investigate the hygroscopic properties of freshly formed nucleation mode particles and grown Aitken mode nucleated particles, respectively.

Because only unimodal size distributions were observed for freshly formed nucleation mode particles (Fig. 2b) and grown Aitken mode particles (Fig. 2c), $g(85\,\%)$ values for these two types of particles were obtained from a Gaussian fit of number size distributions of humidified particles at dry $D_p$ of 20 nm and 40 nm, respectively, during nucleation burst events. Therefore, $g(85\,\%)$ values of freshly formed nucleation mode particles and grown Aitken mode nucleated particles were denoted as $g(85\,\%)_{\_fresh}$ and $g(85\,\%)_{\_Aitken}$, respectively. During the NPF periods at the urban site, $g(85\,\%)_{\_fresh}$ ranged from 1.11 to 1.28 with an average of $1.16 \pm 0.06$, which are equivalent to 1.17 to 1.35 with an average of $1.23 \pm 0.06$ at dry $D_p$ = 100 nm, whereas $g(85\,\%)_{\_Aitken}$ ranged from 1.21 to 1.31 with an average of $1.27 \pm 0.04$, which are equivalent to 1.24 to 1.34 with an average of $1.30 \pm 0.04$ at dry $D_p$ = 100 nm (Table 1).

The $g(85\,\%)$ value of $(NH_4)_2SO_4$ was measured as $1.56 \pm 0.01$ using the H-TDMA used in this study. Laboratory photo-oxidation experiments showed that $g(85\,\%)$ values of the SOA derived from volatile organic compounds were in the range of 1.01–1.16 (Virkkula et al., 1999; Saahoff et al., 2003; Varutbangkul et al., 2006) whereas those of the ambient SOA were obtained as ~ 1.20 (Sjogren et al., 2008; Jung et al., 2011). Average $g(85\,\%)_{\_fresh}$ at the urban site in the present study are much lower than the $g(85\,\%)$ of $(NH_4)_2SO_4$, whereas they are comparable with those of previously studied secondary SOA (Sjogren et al., 2008; Jung et al., 2011). Thus, this result indicates that organic vapors largely contributed to the burst of nucleation mode particles in the Sapporo atmosphere during the summer of 2011.

Average Equiv. $g(85\,\%)_{\_Aitken}$ at dry $D_p$ = 100 nm of grown Aiken mode particles were slightly higher than those of newly formed nucleation mode particles (Table 1), suggesting that the growth of freshly formed nucleation mode particles to the Aitken mode size can be subjected to condensation of not only low-volatility organic vapors





ACPD
14, 8257–8285, 2014



but also water-soluble inorganic compounds. Pavuluri et al. (2013) measured radiocarbon in the water-soluble organic carbon (WSOC) fraction of the aerosols collected at the same urban site. They found that ~ 88 % of WSOC consisted of modern carbon during the summer of 2010. This result indicated that a large fraction of WSOC was originated from biogenic emissions from urban Sapporo and surrounding mixed deciduous forests. Thus, it is suggested that NPF and the subsequent growth of the particles at the urban site are highly affected by biogenic organic emissions.

Ehn et al. (2007) reported the opposite trend in the hygroscopic properties of freshly formed nucleation mode particles in a boreal coniferous forest in southern Finland; they found that the hygroscopic growth factors of freshly formed nucleation mode particles decreased as particles grew to the Aitken mode. The different behaviors of the hygroscopic properties indicate that different growth mechanisms for freshly formed nucleation mode particles may exist between the boreal coniferous forest in southern Finland and the present urban site adjacent to a deciduous forest in northern Japan.

### 3.5 Temporal variations in hygroscopic growth factors of the newly formed particles during the NPF and their subsequent growth event periods

Figure 5 shows temporal variations in number fractions of less-, intermediately-, and highly-hygroscopic particles and $g(85\,\%)$ values at dry $D_p$ of 20 nm and 40 nm during 31 July–2 August and 5–6 August. $g(85\,\%)$ at dry $D_p$ = 20 nm and 40 nm were converted to Equiv. $g(85\,\%)$ at dry $D_p$ = 100 nm by considering the Kelvin Effect. Increased number fractions of intermediately-hygroscopic particles at dry $D_p$ = 20 nm were observed when the burst of nucleation mode particles occurred (Fig. 5a and d), indicating that the hygroscopic property of freshly formed nucleation mode particles is intermediate. High fractions of intermediately-hygroscopic particles were also obtained at dry $D_p$ = 40 nm when the burst of nucleation mode particles and their gradual growth occurred during 31 July, 2 and 5 August under southerly wind condition. This result indicates that the subsequent growth of freshly formed nucleation mode particles was mainly attributed to intermediately-hygroscopic vapors.





ACPD
14, 8257–8285, 2014



Temporal variations in Equiv. $g(85\,\%)$ at dry $D_p = 20$, 40 nm and Mode $D_p$ clearly indicate that the subsequent growth of freshly formed nucleation mode particles and their hygroscopic properties were highly influenced by local wind direction (Fig. 5). Under southerly wind condition during 31 July and 5 August, gradual increases in Mode $D_p$ were obtained with a dominant contribution of intermediately-hygroscopic particles. However, sharp increases in Mode $D_p$ were obtained when wind direction shifted to northwesterly or northeasterly on 1, 2, and 6 August with a sharp increase in highly-hygroscopic particle faction at dry $D_p = 40$ nm. Sudden changes in Mode $D_p$ and hygroscopic growth factor imply that completely different air masses were arrived at the measurement site under northwesterly or northeasterly wind conditions. Thus, local wind direction was an important factor controlling the growth of newly formed particles and their hygroscopic properties.

### 3.6 Hygroscopic properties of large Aitken and accumulation mode particles

Figure 6a shows temporal variations in $N_{nuc}$ and large Aitken to small accumulation modes (80–165 nm) particles ($N_{80-165\,nm}$) during 27 July–8 August. Elevated $N_{nuc}$ were obtained during the NPF event periods. However, different temporal evolutions were obtained for $N_{80-165\,nm}$ with peaks during polluted period (27–29 July and 6–8 August) and clean period (1–5 August). $N_{80-165\,nm}$ ranged from 240 to 1700 particles $cm^{-3}$ with an average of $700 \pm 260$ particles $cm^{-3}$ during the polluted periods, which were approximately 2–3 times higher than those of the clean periods (AVG: $280 \pm 160$ particles $cm^{-3}$, range: 53–1100 particles $cm^{-3}$). Similarly, TSP concentrations during the polluted period ranged from 9 to 80 $\mu g\,m^{-3}$ (AVG $33 \pm 16\,\mu g\,m^{-3}$), which were approximately 2–3 times higher than those (1–48 $\mu g\,m^{-3}$, $14 \pm 9\,\mu g\,m^{-3}$) obtained during the clean period.

Figure 6b and c show air mass backward trajectories arriving at the urban observation site during the polluted and clean periods, respectively. Local wind direction and wind speed during the both periods are also shown in Fig. 6d and e, respectively. Air mass backward trajectories indicate that air masses originating from downwind areas





ACPD
14, 8257–8285, 2014



of the Asian Continent arrived at the urban site during the polluted period (Fig. 6b), whereas air masses originating from the northwestern Pacific arrived during the clean period (Fig. 6c). Local wind direction was also clearly separated between two periods with a dominance of northwesterly winds during the polluted period and southeasterly winds during the clean period. These results suggest that variations in $N_{80-165\,nm}$ are largely affected by the long-range transport of air masses.

Figure 7 shows average number fractions of less-, intermediately-, and highly-hygroscopic particles to total particles at dry $D_p$ = 120 nm as a typical example of the large Aitken to small accumulation mode particles. Number fractions of less-, intermediately-, and highly hygroscopic particles at dry $D_p$ = 120 nm were obtained to be 18 ± 9, 14 ± 8, and 69 ± 14 %, respectively, during the polluted period. However, different number fractions of three hygroscopic particles were obtained during the clean period as 37 ± 14, 17 ± 8, and 46 ± 16 %, respectively (Fig. 7). Significantly higher $g(85\,\%)_{\_total}$ values at dry $D_p$ = 120 nm were obtained during the polluted periods (1.27 ± 0.05) than the clean period (1.19 ± 0.06). In contrast, similar figures were obtained for $g(85\,\%)_{\_more}$ in both periods as shown in Fig. 7. The elevated number fractions of highly-hygroscopic particles and higher $g(85\,\%)_{\_total}$ values at dry $D_p$ = 120 nm during the polluted period compared to the clean period imply that air masses originating from downwind areas of the Asian Continent contain high abundances of highly-hygroscopic Aitken to accumulation mode particles.

The number concentrations of less-hygroscopic particles at the dry $D_p$ range of 40–120 nm increased during early morning and evening with the exception of dry $D_p$ = 20 nm (Fig. 2). Figure 8 shows diel variations in the number concentrations of less-hygroscopic particles at dry $D_p$ = 100 nm and NO concentrations. Diel variations in the number concentrations of less-hygroscopic particles showed two peaks at 07:00–08:00 LT and 19:00–20:00 LT. NO concentrations showed a similar diel variation with a major peak at 08:00–09:00 LT and a minor peak at 18:00 LT. These results imply that less-hygroscopic particles might be directly emitted from local anthropogenic activities such as traffic and cooking activities.





ACPD
14, 8257–8285, 2014



## 4 Summary and conclusions

The burst of nucleation mode particles and $g(85\,\%)_{\_total}$ values at the dry $D_p$ range of 20–120 nm were characterized by three phases: small increases in $N_{nuc}$ and sharp decreases in $g(85\,\%)$ values during 05:00–08:00 LT, sharp increases in $N_{nuc}$ and $g(85\,\%)$ during 08:00–10:30 LT, and peak $N_{nuc}$ and relatively constant $g(85\,\%)_{\_total}$ values during 10:30–12:00 LT. Small increases in $N_{nuc}$ and sharp decreases in $g(85\,\%)$ together with large increases in NO concentrations during 05:00–08:00 LT suggest that water-insoluble particles from traffic are important to lower the hygroscopicity of ultrafine particles prior to the burst of nucleation mode particles. Sharp increases in both $N_{nuc}$ and $g(85\,\%)$ with simultaneous increases in $SO_2$ and $O_3$ concentrations during 08:00–10:30 LT may indicate that freshly formed nucleation mode particles are enriched with water-soluble components. The equivalent $g(85\,\%)$ values of freshly formed nucleation mode particles at the urban site were obtained as 1.17–1.35 (avg. $1.23 \pm 0.06$). These hygroscopic growth factors are similar to those of secondary organic aerosols, suggesting that low-volatility organic vapors are important to the burst of nucleation mode particles.

Diel variations in less-hygroscopic particles were strongly correlated with NO concentrations, suggesting that less-hygroscopic particles are mainly produced from anthropogenic activities such as traffic. The $g(85\,\%)$ values of total particles at dry $D_p$ = 120 nm were measured to be $1.27 \pm 0.05$ when air masses originating from downwind areas of the Asian Continent arrived to the urban site, being higher than those ($1.19 \pm 0.06$) under marine air mass conditions. These results indicate that the hygroscopic property of large Aitken and small accumulation mode particles (80–165 nm) at the urban site are highly influenced by the long-range transport of atmospheric particles from the Asian Continent.

Organic vapors in the urban atmosphere are generally emitted from anthropogenic and biogenic sources. They also can be transported from surrounding forests. To better understand the effects of biogenic organic emissions on NPF and their subsequent





ACPD
14, 8257–8285, 2014



growth mechanism in urban Sapporo, apportionment of particulate organic aerosols into anthropogenic and biogenic origins is necessary. This apportionment can be accomplished by measurements of radiocarbon and biogenic SOA tracers in sub-μm particles (Pavuluri et al., 2013). Further investigations of diel variations in biogenic SOA tracers and radiocarbon isotopic ratios of nucleated particles are necessary to better understand an interaction between biogenic and anthropogenic emissions and their effects on NPF and the subsequent growth of freshly nucleated particles.

*Acknowledgements.* This work was in part supported by Grant-in-Aid nos. 2100923509 and 24221001 from the Japan Society for the Promotion of Science (JSPS) and by the Environment Research and Technology Development Fund (B-0903) of the Ministry of the Environment, Japan. We appreciate the financial support of a JSPS Fellowship to J. S. Jung. We acknowledge to the Ministry of the Environment of Japan and Japan Meteorological Agency for their criteria pollutants and meteorological parameters, respectively.

## References

Aggarwal, S. G. and Kawamura, K.: Carbonaceous and inorganic composition in long-range transported aerosols over northern Japan: implication for aging of water-soluble organic fraction, Atmos. Environ., 43, 2532–2540, 2009.

Agarwal, S., Aggarwal, S. G., Okuzawa, K., and Kawamura, K.: Size distributions of dicarboxylic acids, ketoacids, $\alpha$-dicarbonyls, sugars, WSOC, OC, EC and inorganic ions in atmospheric particles over Northern Japan: implication for long-range transport of Siberian biomass burning and East Asian polluted aerosols, Atmos. Chem. Phys., 10, 5839–5858, doi:10.5194/acp-10-5839-2010, 2010.

Bzdek, B. R. and Johnston, M. V.: New particle formation and growth in the troposphere, Anal. Chem., 82, 7871–7878, 2010.

Cheung, H. C., Morawska, L., and Ristovski, Z. D.: Observation of new particle formation in subtropical urban environment, Atmos. Chem. Phys., 11, 3823–3833, doi:10.5194/acp-11-3823-2011, 2011.

Clegg, S. L., Brimblecombe, P., and Wexler, A. S.: Thermodynamic model of the system $H^+$-$NH_4^+$-$Na^+$-$SO_4^{2-}$-$NO_3^-$-$Cl^-$-$H_2O$ at 298.15 K, J. Phys. Chem. A, 102, 2155–2171, 1998.





ACPD
14, 8257–8285, 2014



Draxler, R. R. and Rolph, G. D.: HYSPLIT (HYbrid Single-Particle Lagrangian Integrated Trajectory) Model access via NOAA ARL READY Website (http://www.arl.noaa.gov/HYSPLIT.php), NOAA Air Resources Laboratory, Silver Spring, MD, 2012.

Ehn, M., Petäjä, T., Aufmhoff, H., Aalto, P., Hämeri, K., Arnold, F., Laaksonen, A., and Kulmala, M.: Hygroscopic properties of ultrafine aerosol particles in the boreal forest: diurnal variation, solubility and the influence of sulfuric acid, Atmos. Chem. Phys., 7, 211–222, doi:10.5194/acp-7-211-2007, 2007.

Ehn, M., Thornton, J. A., Kleist, E., Sipilä, M., Junninen, H., Pullinen, I., Springer, M., Rubach, F., Tillmann, R., Lee, B., Lopez-Hilfiker, F., Andres, S., Acir, I.-H., Rissanen, M., Jokinen, T., Schobesberger, S., Kangasluoma, J., Kontkanen, J., Nieminen, T., Kurtén, T., Nielsen, L. B., Jørgensen, S., Kjaergaard, H. G., Canagaratna, M., Dal Maso, M., Berndt, T., Petäjä, T., Wahner, A., Kerminen, V., Kulmala, M., Worsnop, D. R., Wildt, J., and Mentel, T. F.: A large source of low-volatility secondary organic aerosol, Nature, 506, 476–479, doi:10.1038/nature13032, 2014.

Gao, J., Wang, T., Zhou, X., Wu, W., and Wang, W.: Measurement of aerosol number size distributions in the Yangtze River delta in China: formation and growth of particles under polluted conditions, Atmos. Environ., 43, 829–836, 2009.

Gysel, M., Weingartner, E., Nyeki, S., Paulsen, D., Baltensperger, U., Galambos, I., and Kiss, G.: Hygroscopic properties of water-soluble matter and humic-like organics in atmospheric fine aerosol, Atmos. Chem. Phys., 4, 35–50, doi:10.5194/acp-4-35-2004, 2004.

Hegg, D. A. and Baker, M. B.: Nucleation in the atmosphere, Rep. Prog. Phys., 72, 056801, doi:10.1088/0034-4885/72/5/056801, 2009.

Holmes, N. S.: A review of particle formation events and growth in the atmosphere in the various environments and discussion of mechanistic implications, Atmos. Environ., 41, 2183–2201, 2007.

Jung, J., Kim, Y. J., Aggarwal, S. G., and Kawamura, K.: Hygroscopic property of water-soluble organic-enriched aerosols in Ulaanbaatar, Mongolia during the cold winter of 2007, Atmos. Environ., 45, 2722–2729, 2011.

Jung, J., Miyazaki, Y., and Kawamura, K.: Different characteristics of new particle formation between urban and deciduous forest sites in Northern Japan during the summers of 2010–2011, Atmos. Chem. Phys., 13, 51–68, doi:10.5194/acp-13-51-2013, 2013.





ACPD
14, 8257–8285, 2014



Kitamori, Y., Mochida, M., and Kawamura, K.: Assessment of the aerosol water content in urban atmospheric particles by the hygroscopic growth measurements in Sapporo, Japan, Atmos. Environ., 43, 3416–3423, 2009.
Kulmala, M., Vehkamäki, H., Petäjä, Dal Maso, T. M., Lauri, A., Kerminen, V.-M., Birmili, W., and McMurry, P. H.: Formation and growth rates of ultrafine atmospheric particles: a review of observations, J. Aerosol Sci., 35, 143–176, 2004.
Kulmala, M., Kontkanen, J., Junninen, H., Lehtipalo, K., Manninen, H. E., Nieminen, T., Petäjä, T., Sipilä, M., Schobesberger, S., Rantala, P., Franchin, A., Jokinen, T., Järvinen, E., Äijälä, M., Kangasluoma, J., Hakala, J., Aalto, P.P, Paasonen, P., Mikkilä, J., Vanhanen, J., Aalto, J., Hakola, H., Makkonen, U., Ruuskanen, T., Mauldin, R. L., Duplissy, J., Vehkamäki, H., Bäck, J., Kortelainen, A., Riipinen, I., Kúrten, T., Johnston, M. V., Smith, J. N., Ehn, M., Mentel, T. F., Lehtinen, K. E. J., Laaksonen, A., Keminen, V.-M., and Worsnop, D.: Direct observations of atmospheric aerosol nucleation, Science, 339, 943–946, doi:10.1126/science.1227385, 2013.
Kuwata, M., Kondo, Y., Mochida, M., Takegawa, N., and Kawamura, K.: Dependence of CCN activity of less volatile particles on the amount of coating observed in Tokyo, J. Geophys. Res., 112, D11207, doi:10.1029/2006JD007758, 2007.
Metzger, A., Verheggen, B., Dommen, J., Duplissy, J., Prevot, A. S., Weingartner, E., Riipinen, I., Kulmala, M., Spracklen, D. V., Carslaw, K. S., and Baltensperger, U.: Evidence for the role of organics in aerosol particle formation under atmospheric conditions, P. Natl. Acad. Sci. USA, 107, 6646–6651, 2010.
Mochida, M. and Kawamura, K.: Hygroscopic properties of levoglucosan and related organic compounds characteristic to biomass burning aerosol particles, J. Geophys. Res., 109, D21202, doi:10.1029/2004JD004962, 2004.
Mochida, M., Miyakawa, T., Takegawa, N., Morino, Y., Kawamura, K., and Kondo, Y.: Significant alteration in the hygroscopic properties of urban aerosol particles by the secondary formation of organics, Geophys. Res. Lett., 35, L02804, doi:10.1029/2007GL031310, 2008.
Pavuluri, C. M., Kawamura, K., Uchida, M., Kondo, M., and Fu, P.: Enhanced modern carbon and biogenic organic tracers in Northeast Asian aerosols during spring/summer, J. Geophys. Res., 118, 2362–2371, doi:10.1002/jgrd.50244, 2013.
Ristovski, Z. D., Suni, T., Kulmala, M., Boy, M., Meyer, N. K., Duplissy, J., Turnipseed, A., Morawska, L., and Baltensperger, U.: The role of sulphates and organic vapours in growth





ACPD
14, 8257–8285, 2014



of newly formed particles in a eucalypt forest, Atmos. Chem. Phys., 10, 2919–2926, doi:10.5194/acp-10-2919-2010, 2010.
Rolph, G. D.: Real-time Environmental Applications and Display sYstem (READY) Website (http://www.arl.noaa.gov/ready.php), NOAA Air Resources Laboratory, Silver Spring, MD, 2012.
Saathoff, H., Naumann, K. H., Schnaiter, M., Schock, W., Mohler, O., Schurath, U., Weingartner, E., Gysel, M., and Baltensperger, U.: Coating of soot and $(NH_4)_2SO_4$ particles by ozonolysis products of alpha-pinene, J. Aerosol Sci., 34, 1297–1321, 2003.
Sjogren, S., Gysel, M., Weingartner, E., Alfarra, M. R., Duplissy, J., Cozic, J., Crosier, J., Coe, H., and Baltensperger, U.: Hygroscopicity of the submicrometer aerosol at the high-alpine site Jungfraujoch, 3580 m a.s.l., Switzerland, Atmos. Chem. Phys., 8, 5715–5729, doi:10.5194/acp-8-5715-2008, 2008.
Stohl, A.: Computation, accuracy and applications of trajectories: a review and bibliography, Atmos. Environ., 32, 947–966, 1998.
Varutbangkul, V., Brechtel, F. J., Bahreini, R., Ng, N. L., Keywood, M. D., Kroll, J. H., Flagan, R. C., Seinfeld, J. H., Lee, A., and Goldstein, A. H.: Hygroscopicity of secondary organic aerosols formed by oxidation of cycloalkenes, monoterpenes, sesquiterpenes, and related compounds, Atmos. Chem. Phys., 6, 2367–2388, doi:10.5194/acp-6-2367-2006, 2006.
Virkkula, A., Van Dingenen, R., Raes, F., and Hjorth, J.: Hygroscopic properties of aerosol formed by oxidation of limonene, alpha-pinene, and beta-pinene, J. Geophys. Res., 104, 3569–3579, 1999.
Yue, D. L., Hu, M., Zhang, R. Y., Wang, Z. B., Zheng, J., Wu, Z. J., Wiedensohler, A., He, L. Y., Huang, X. F., and Zhu, T.: The roles of sulfuric acid in new particle formation and growth in the mega-city of Beijing, Atmos. Chem. Phys., 10, 4953–4960, doi:10.5194/acp-10-4953-2010, 2010.
Zhang, R.: Getting to the critical nucleus of aerosol formation, Science, 328, 1366–1367, 2010.
Zhang, R., Khalizov, A., Wang, L., Hu, M., and Xu, W.: Nucleation and growth of nanoparticles in the atmosphere, Chem. Rev., 112, 1957–2011, 2012.





ACPD
14, 8257–8285, 2014



**Table 1.** Summary of *Mode* $D_p$ and $g(85\,\%)$ values of freshly formed nucleation mode particles and grown Aitken mode nucleated particles at the urban site.

| Date | Freshly formed nucleation mode particles | | | Grown Aitken mode nucleated particles | | |
|---|---|---|---|---|---|---|
| | Mode $D_p$ (nm) | $g(85\,\%)$ at dry $D_p$ = 20 nm[a] | Equiv. $g(85\,\%)$ at dry $D_p$ = 100 nm[b] | Mode $D_p$ (nm) | $g(85\,\%)$ at dry $D_p$ = 40 nm[c] | Equiv. $g(85\,\%)$ at dry $D_p$ = 100 nm[b] |
| 27 Jul 2011 | 24 | 1.28 | 1.35 | 44 | 1.31 | 1.34 |
| 31 Jul 2011 | 12 | 1.12 | 1.19 | | | |
| 1 Aug 2011 | 14 | 1.11 | 1.17 | 48 | 1.26 | 1.29 |
| 2 Aug 2011 | 15 | 1.17 | 1.24 | | | |
| 3 Aug 2011 | 14 | 1.12 | 1.19 | | | |
| 5 Aug 2011 | 13 | 1.11 | 1.17 | | | |
| 6 Aug 2011 | 22 | 1.22 | 1.29 | 47 | 1.28 | 1.31 |
| 8 Aug 2011 | 18 | 1.16 | 1.23 | 38 | 1.21 | 1.24 |
| Min | 12 | 1.11 | 1.17 | 38 | 1.21 | 1.24 |
| Max | 24 | 1.28 | 1.35 | 48 | 1.31 | 1.34 |
| AVG | 16 | 1.16 | 1.23 | 44 | 1.27 | 1.3 |
| S.D. | 4.0 | 0.06 | 0.6 | 4.5 | 0.04 | 0.04 |

[a] $g(85\,\%)$ at dry $D_p$ = 20 nm represent the $g(85\,\%)$ of freshly formed nucleation mode particles.

[b] $g(85\,\%)$ at dry $D_p$ = 20 and 40 nm were converted to Equiv. $g(85\,\%)$ of dry $D_p$ = 100 nm by considering the Kelvin Effect.

[c] $g(85\,\%)$ at dry $D_p$ = 40 nm represent the $g(85\,\%)$ of grown Aitken mode nucleated particles.





ACPD
14, 8257–8285, 2014



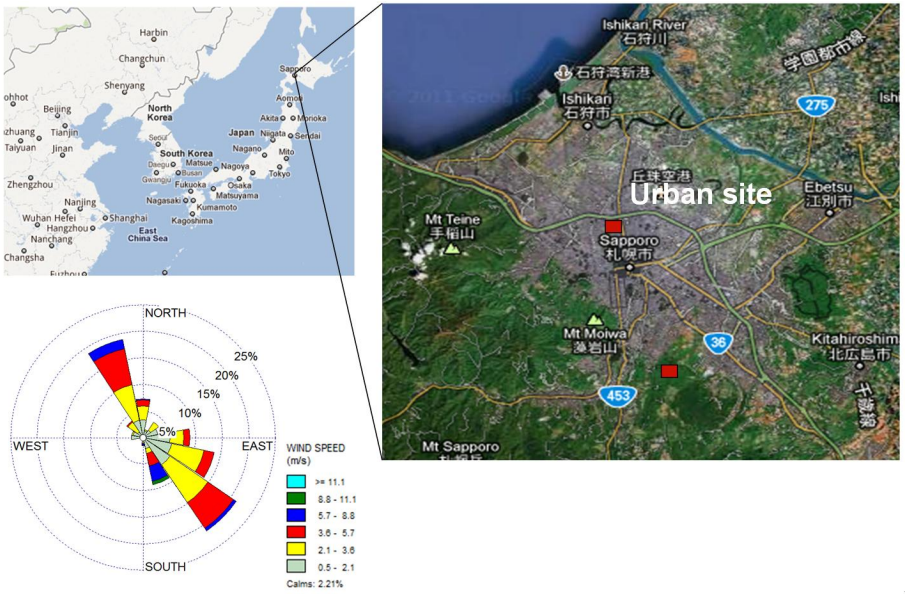


**Fig. 1.** Image map of a measurement site. The urban site is located at the north campus of Hokkaido University (43°3′56″ N, 141°21′27″ E) in the northwest of downtown Sapporo, northern Japan. Observed frequencies of local wind direction with wind speed are also shown.





ACPD
14, 8257–8285, 2014



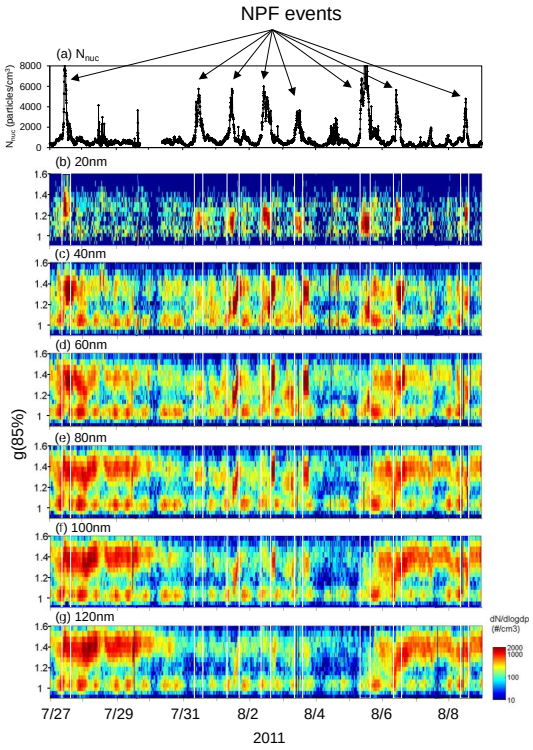


**Fig. 2.** Temporal evolutions of **(b–g)** the number concentrations of atmospheric particles as a function of hygroscopic growth factor at 85 % RH ($g$(85 %)) at the urban site during 27 July–8 August 2011. The number concentrations of nucleation mode (7–30 nm) particles ($N_{nuc}$) are also shown in **(a)**. Dry particle diameter ($D_p$) increases from **(b)** 20 nm to **(g)** 120 nm with a 20 nm increment. Eight new particle formation (NPF) event days were characterized on 27, 31 July and 1–3, 5, 6, 8 August 2011 as marked by white boxes.





ACPD
14, 8257–8285, 2014



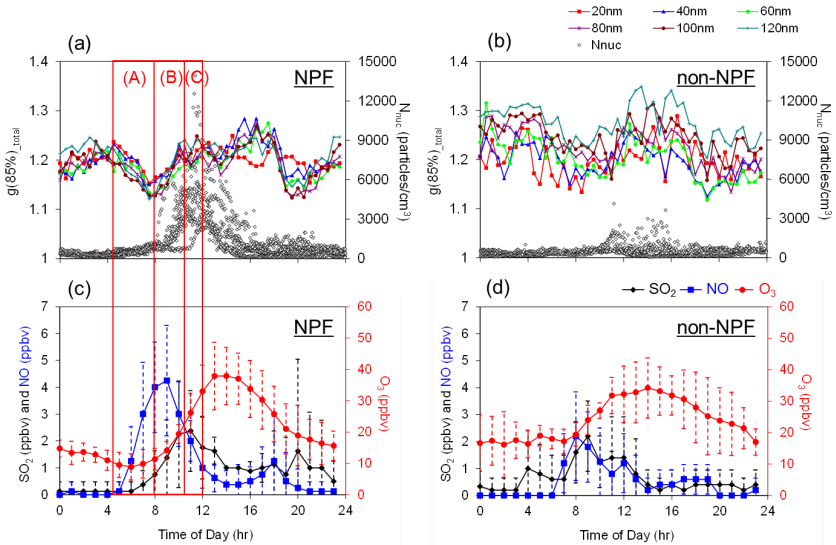


**Fig. 3.** Diel variations in **(a, b)** median $g(85\,\%)$ values at the dry $D_p$ range of 20–120 nm with a 20 nm increment, $N_{nuc}$, **(c, d)** $SO_2$, NO, and $O_3$ concentrations during the NPF event **(a, c)** and non-NPF **(b, d)** periods. $g(85\,\%)$ at dry $D_p$ = 20, 40, 60, 80 nm were converted to Equiv. $g(85\,\%)$ of dry $D_p$ = 100 nm by considering the Kelvin Effect.





ACPD
14, 8257–8285, 2014



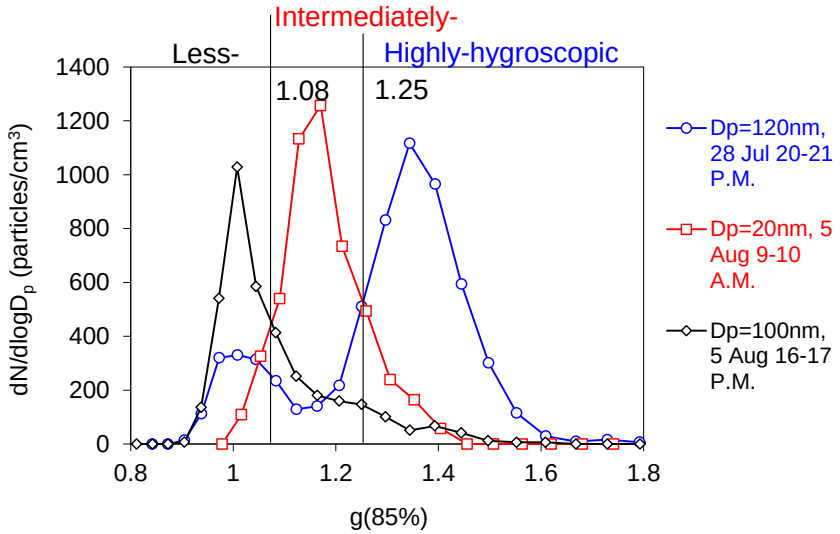


**Fig. 4.** Log-normal number distributions of humidified particles as a function of $g$(85 %) values on 5 August 16:00–17:00 LT at dry $D_p$ = 100 nm, 5 August 09:00–10:00 LT at dry $D_p$ = 20 nm, and 28 July 20:00–21:00 LT at $D_p$ = 120 nm as typical examples for less-, intermediately-, and highly-hygroscopic particles, respectively. Vertical lines at g(85 %) values of 1.08 and 1.25 represent threshold values between less-, intermediately-, and highly-hygroscopic fractions. $g$(85 %) at dry $D_p$ = 20 nm was converted to Equiv. $g$(85 %) of dry $D_p$ = 100 nm by considering the Kelvin Effect.





ACPD
14, 8257–8285, 2014



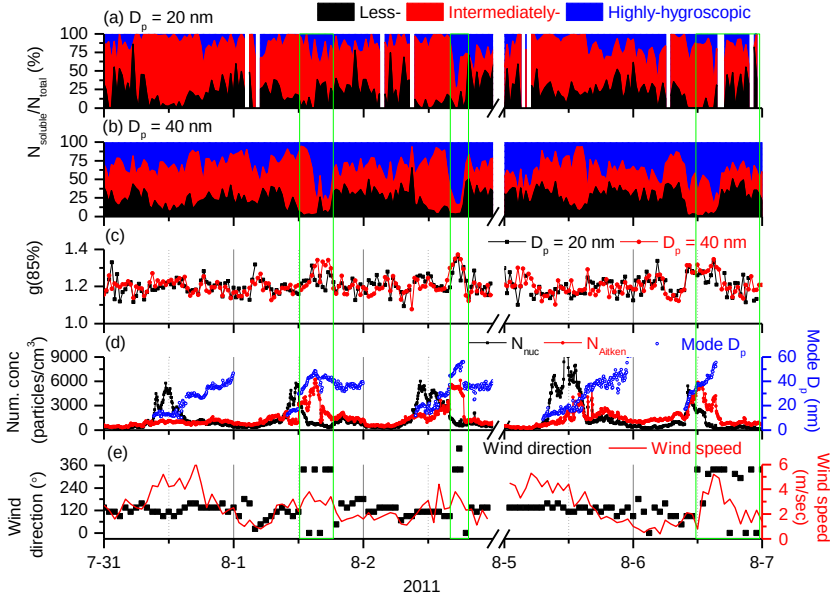


**Fig. 5.** Temporal variations in number fractions of less-, intermediately-, and highly-hygroscopic particles at **(a)** dry $D_p$ values of 20 nm and **(b)** 40 nm, **(c)** $g$(85 %) values of total particles at dry $D_p$ values of 20 nm and 40 nm, **(d)** $N_{nuc}$ and Aitken (30–100 nm) mode particles ($N_{Aitken}$) and Mode $D_p$ during 31 July–2 August and 5–6 August. **(e)** Temporal variations in wind direction and wind speed are also shown. $g$(85 %) at dry $D_p$ = 20, 40 nm were converted to Equiv. $g$(85 %) of dry $D_p$ = 100 nm by considering the Kelvin Effect.





ACPD
14, 8257–8285, 2014



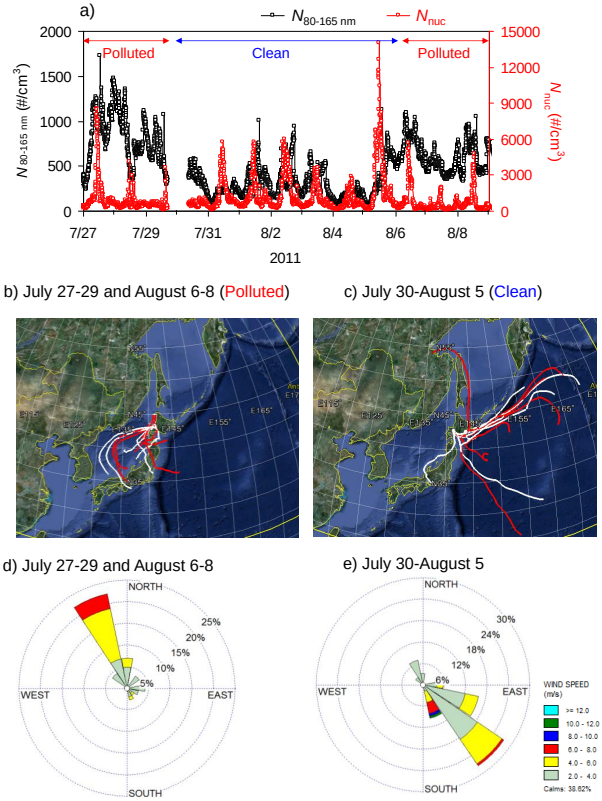


**Fig. 6. (a)** Integrated number concentrations of particles from 80 nm to 165 nm ($N_{80-165\,nm}$) and $N_{nuc}$ during the entire measurement period and air mass backward trajectories arriving at the urban site and observed frequencies of local wind direction with wind speed during **(b, d)** 27–29 July and 6–8 August 2011 (Polluted) and **(c, e)** 30 July–5 August (Clean). White and red trajectories in **(b)** and **(c)** represent air mass trajectories arriving at 200 m and 500 nm heights above ground level, respectively.





ACPD
14, 8257–8285, 2014



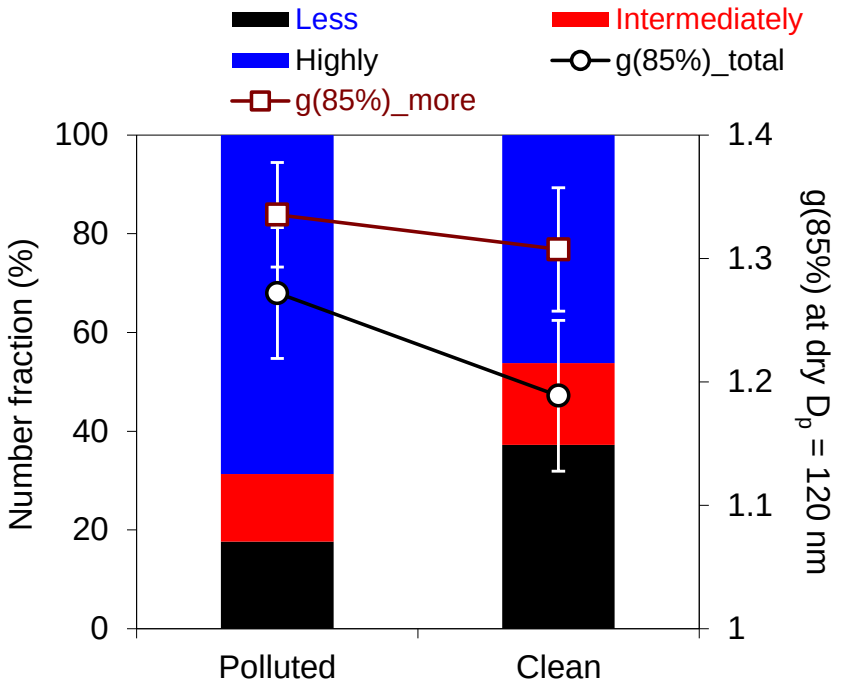


**Fig. 7.** Average number fractions of less-, intermediately-, and highly-hygroscopic particles at dry $D_p$ values of 120 nm during the Polluted and Clean periods. $g(85\,\%)$ values of total particles ($g(85\,\%)_{\_total}$) and more-hygroscopic particles ($g(85\,\%)_{\_more}$) are also shown. The more-hygroscopic particles are defined as a sum of intermediately- and highly-hygroscopic particles.





ACPD
14, 8257–8285, 2014



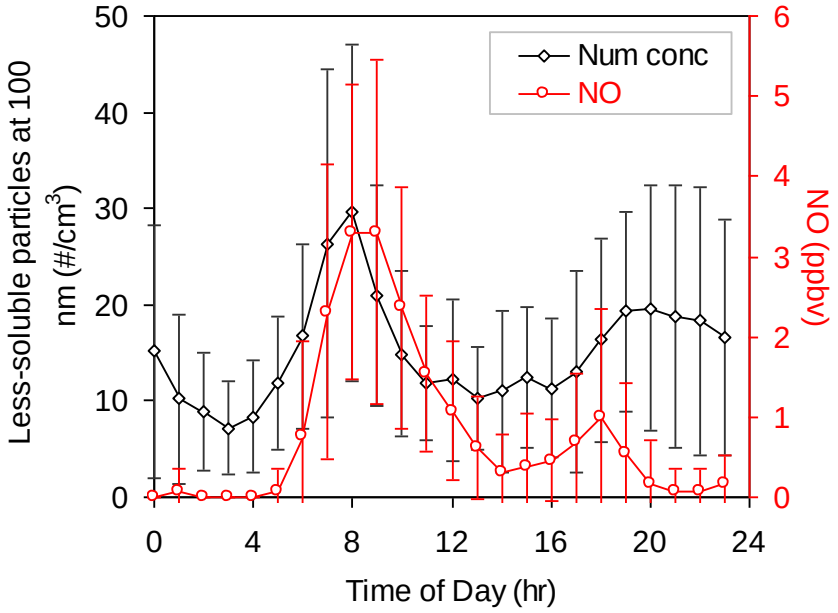


**Fig. 8.** Diel variations in less-hygroscopic particles at dry $D_p$ = 100 nm and NO concentrations during the entire measurement periods.





ACPD
14, 8257–8285, 2014